MECH-124

Contract N00014-86-K-0753

CRACK-GROWTH RESISTANCE IN TRANSFORMATION-TOUGHENED CERAMICS

DAVID M. STUMP and BERNARD BUDIANSKY

Division of Applied Sciences
HARVARD UNIVERSITY
Cambridge, Massachusetts 02138

June 1988

CRACK- GROWTH RESISTANCE IN TRANSFORMATION-TOUGHENED CERAMICS

David M. Stump and Bernard Budiansky
Division of Applied Sciences
Harvard University
Cambridge, MA 02138

June 1988

ABSTRACT

Crack-growth resistance in transformation-toughened ceramics is studied by modeling the region surrounding an advancing crack tip as a zone which has undergone a uniform dilatational phase transformation. This zone is allowed to evolve around the advancing crack tip under conditions of increasing far-field load while the tip is maintained at a critical stress intensity necessary for fracture. This procedure leads to the surprising conclusion that maximum toughening occurs for finite amounts of crack advance.

INTRODUCTION

The discovery of enhanced fracture toughness in *zirconia-enriched ceramics* has led to a flurry of experimental and theoretical analyses. It has been well established that the high stresses near a crack tip can cause small zirconia particles, typically one micron or less in diameter, to undergo a phase transformation from a tetragonal to a monoclinic crystal structure. The unconstrained transformation can be decomposed into a four percent dilatation and a sixteen percent shear strain. However , due to the elastic constraint of the matrix phase, the particles in the composite generally transform with twin bands of alternate character resulting in an overall transformation strain considerably less than sixteen percent. Consequently, the strain transformation of particles embedded in the composite is usually assumed to be dilatant.

The transformed region has the remarkable property of allowing stable crack growth to occur in the composite material, whereas the unreinforced ceramic exhibits no such behavior. Stable crack growth on the order of several millimeters has been observed, and R-curves (i.e. stress intensity versus crack extension) for a variety of zirconia-reinforced composites have been measured.

Theoretical studies of transformation toughening including those of McMeeking and Evans (1982), Budiansky et al. (1983), Amazigo and Budiansky (1987), Rose (1986a) and Lambropoulos (1986) have considered only steady-state toughening, wherein a semi-infinite planar crack is surrounded by a semi-infinite zone of dilatation, as shown in Fig. 1a. Using a primitive analysis, Rose (1986b) also examined the effect of allowing an initial transformation zone to grow with an advancing crack tip. The objective of this study is to present a complete analysis of the growing crack by solving for the initial transformation zone and studying its growth around a crack tip advancing under increasing, far field, Mode-I loading. This analysis will reveal the surprising result that maximum toughening occurs for a finite amount of crack advance.

INITIAL ZONES

The modeling approach adopted in this study, consistent with previous work, is to assume that a transformation zone surrounding the initial crack tip has undergone an irreversible transformation dilatation of strength $c\theta_p^T$, as shown in Fig. 1b, where c is the zirconia particle volume fraction and θ_p^T is the unconstrained particle dilatation. The crack will be taken to be semi-infinite and planar. The transformed and untransformed regions will be assumed to have the same elastic moduli, and to be under plane strain.

Since typical zone sizes are of the order of 20 μm or less, small compared to specimen dimensions, the small scale zone-size approximation will be invoked. The stresses at distances far from the zone, but small compared to the size of the body, will be assumed to be dominated by the classic Mode I K-field . For $r \to \infty$, the stresses $\sigma_{\alpha\beta}$ are given by

$$\sigma_{\alpha\beta} = \frac{K}{\sqrt{2\pi r}} F_{\alpha\beta}(\phi) \tag{1}$$

where the $F_{\alpha\beta}(\phi)$ are well known trigonometric functions and K is the applied far-field stress intensity. Similarly, in the vicinity of the crack tip, $r \to 0$, the stresses are given by

$$\sigma_{\alpha\beta} = \frac{K_{tip}}{\sqrt{2\pi r}} F_{\alpha\beta}(\phi) \tag{2}$$

where K_{tip} is the stress intensity at the crack tip.

The full transformation will be assumed to occur when the mean stress, $\sigma_m = \sigma_{kk}/3$, attains a critical value σ_m^c. This corresponds to the "supercritical" transformation case considered by Budiansky et al. (1983). The value of σ_m^c, as discussed by Evans and Cannon (1986), will depend on the stress and temperature history of the composite. Other transformation criteria have also been proposed (Lambropoulos 1986).

As shown by Budiansky et al., the application of the J-integral to the stationary crack results in the conclusion that $K_{tip} = K$. Accordingly, if crack growth occurs at a critical stress intensity, $K_{tip} = K_m$, where K_m is independent of the particle concentration, the initial transformation region induces no toughening. This neglects the possible effects of other toughening mechanisms such as microcracking.

To determine the boundary of the initial transformation zone (Fig. 1b), it is necessary to insist that the mean stress σ_m attain the value σ_m^c as the boundary is approached from the exterior of the zone. By the superposition of stresses, the mean stress exterior to the zone boundary is the sum of contributions from the applied far-field and from dilatations in the transformed region.

The mean stress due to the far-field stresses of eqn (1) is

$$\sigma_m = \frac{K(1+\nu)}{3}\left(\frac{\pi r}{2}\right)^{-1/2}\cos(\phi/2) \tag{3}$$

The mean stress contribution of the transformed zone can be found by first considering that due to the two small circular spots of dilatation shown in Fig. 2. For spots of area dA_0, strength $c\theta_p^T$, and located at $z_0 = x_0+iy_0$ and $\bar{z}_0 = x_0-iy_0$, the mean stress as found by Hutchinson (1974) is

$$\sigma_m = \frac{Ec\theta_p^T}{18\pi}\left[\frac{1+\nu}{1-\nu}\right]\mathrm{Re}\left\{\frac{1}{\sqrt{zz_0}\left[\sqrt{z}+\sqrt{z_0}\right]}+\frac{1}{\sqrt{z\bar{z}_0}\left[\sqrt{z}+\sqrt{\bar{z}}\right]}\right\}dA_0 \tag{4}$$

The spots at z_0 and $\bar{z}_0$ induce a change in tip stress intensity

$$\Delta K_{tip} = \frac{Ec\theta_p^T}{6\sqrt{2\pi}\,(1-\nu)}\mathrm{Re}\left[z_0^{-3/2}+\bar{z}_0^{-3/2}\right]dA_0 \tag{5}$$

Rewriting eqn (5) in terms of polar coordinates r and ϕ, yields the equivalent form,

$$\Delta K_{tip} = \frac{Ec\theta_p^T}{3\sqrt{2\pi}\,(1-\nu)}\, r^{-3/2} \cos(3\phi/2) dA_0 \tag{6}$$

Transformations in the region $\phi < \pi/3$ increase K_{tip}, while those in the region $\phi > \pi/3$ decrease K_{tip}.

The effect of the entire zone on the mean stress can be calculated by integrating eqn (4) over the upper half A of the transformed zone (Fig. 1b). The equation for the zone boundary is then obtained by adding the far field mean stress to the zone contribution and equating the sum to σ_m^c. Thus, the equation governing points $z = R(\phi)e^{i\phi}$ on the boundary is

$$\sigma_m^c = \frac{K(1+\nu)}{3}\left(\frac{\pi R}{2}\right)^{-1/2} \cos(\phi/2) + \int\int_A F(z,z_0)dx_0dy_0 \tag{7}$$

where $F(z,z_0)$ is given by eqn (4).

Carrying out the integration with respect to dx_0 and setting $K = K_m$ leads to the following condition governing $R(\phi)$ when crack growth is imminent:

$$1 = \left(\frac{L}{R(\phi)}\right)^{1/2} \cos(\phi/2) - \frac{\omega}{9\pi}\int_0^{\pi} M(\phi,\phi')\,\frac{dy_0(\phi')}{L} \tag{8}$$

where

$$M(\phi,\phi') = Re\left\{\frac{L}{\sqrt{z}\left[\sqrt{z}+\sqrt{z_0}\right]} + \frac{L}{\sqrt{z}\left[\sqrt{z}+\sqrt{\bar{z}_0}\right]}\right\} \tag{9}$$

with $\quad z = R(\phi)e^{i\phi}\,,\; z_0 = R(\phi')e^{i\phi'}\,.$

Here the parameter ω, defined by

$$\omega = \frac{Ec\theta_p^T}{\sigma_m^c}\left[\frac{1+\nu}{1-\nu}\right] \tag{10}$$

is a non-dimensional measure of the strength of the transformation, and the characteristic length L is

$$L = \frac{2}{9\pi}\left[\frac{K_m(1+\nu)}{\sigma_m^c}\right]^2 \tag{11}$$

Note that L is the frontal intercept at $\phi = 0$ of the σ_m^c boundary for $\omega = 0$.

The stress intensity at the tip is equal to the sum of the applied stress intensity and that induced by the presence of the transformation zone. Integrating eqn (5) over upper half of the zone and adding the applied far-field intensity results in the equation

$$K_{tip} = K + \frac{Ec\theta_p^T}{6\sqrt{2\pi}\,(1-\nu)} \int\int_A (z_0^{-3/2} + \bar{z}_0^{-3/2})\, dx_0 dy_0 \qquad (12)$$

for K_{tip}. Integrating with respect to dx_0 results in the equation

$$\frac{K_{tip}}{K_m} = \frac{K}{K_m} - \frac{2\omega}{9\pi} \int_0^{\pi} \left(\frac{R}{L}\right)^{-1/2} \cos(\phi/2)\, \frac{dy_0(\phi)}{L} \qquad (13)$$

But, for the initial crack, $K_{tip} = K$, and for crack growth to occur $K_{tip} = K_m$. Hence, eqn (13) with $K_{tip}/K_m = K/K_m = 1$ serves as a check on the solution of (8) for the initial boundary curve $R(\phi)$.

The procedure used to solve eqn (8) for $R(\phi)/L$ is described in appendix A and the results for various values of ω ranging from 0 to 30 are shown in Fig. 3. The effect of increased ω on the relative shapes of the zones can be seen in Fig. 4, where for each ω all distances have been normalized by the frontal intercept R(0).

Figure 5 shows the initial zone-heights of Fig. 3, together with the zone-heights corresponding to steady-state crack growth calculated by Budiansky and Amazigo (1987). For $\omega = 30$, the steady state zone height becomes infinite, corresponding to the "lock-up" -- i.e. infinite toughening -- discovered by Rose (1986b)

GROWING CRACKS

Once the initial zone has been found, it is possible to contemplate its growth around an advancing crack tip. As a growing crack moves into the body, material in the vicinity of the tip attains the critical mean stress and transforms, while due to the irreversibility of the transformation a wake region is left behind. Along a frontal portion of the transformed-zone boundary the mean stress criterion is satisfied, while on the wake portion of the boundary the mean stress will have dropped below σ_m. According to eqn (6) material in the transformed region which lies to the left

of the radial line running through the tip at the angle $\pi/3$ reduces the stress intensity at the tip. To continue driving the crack forward, the applied stress intensity must be incremented. Consequently to solve the growing crack problem, both the stress intensity and zone shape must be found as functions of crack extension.

The upper half of the instantaneous zone around a growing crack is shown in Fig. 6a. The boundary is modeled by three segments; active, passive, and residual. The active segment AB is that portion of the boundary where the mean stress has just reached σ_m^c. The mean stress on the remainder of the boundary has dropped below σ_m^c. The residual segment CD is the portion of the initial boundary left behind with the first increment of crack growth. The intermediate passive portion BC is a growth dependent piece connecting the active and residual segments. The passive portion is comprised entirely of the end points B of previous active segments, several of which are shown in the sketch.

The solution for the growing crack problem involves adapting the three segment approach to a series of finite crack increments. In the limit of continuous crack advance, the passive segment provides a smooth connection from the residual portion to the instantaneous active segment. However for a series of finite crack increments, a piecewise linear approximation to the passive zone can be constructed by connecting the residual segment to the currently active segment with a series of straight lines running through the end points of previous active pieces. In the limit of infinitesimal crack increments the approximate boundary should coincide with the actual passive segment.

The setup for a typical growth increment Δa is shown in Fig. 6b. The active segment AB is described with respect to moving crack tip coordinates r and ϕ, where ϕ is assumed to span the angular interval from 0 to an unknown angle α. For the growth increment Δa the passive segment extension is modeled by using a straight line to connect the end of the instantaneous active segment, B, to B', the end of the previous active segment. Tangency between the active and passive segments at B is enforced. For the first crack increment, the passive segment connection with the initial zone shape must also be found. As shown in Fig. 6b, the passive-residual

boundary at C will be described by the unknown angle β, measured with respect to the initial crack position. Tangency between the residual and passive segments will also be enforced at point C.

The analysis presented for the initial crack problem can be applied to the growing crack configuration with some slight modifications. The initial zone will be allowed to grow with an advancing crack tip under the dual requirements of satisfying the critical mean stress condition on the active zone boundary and maintaining the tip stress intensity at K_m.

The mean stress criterion, eqn (7), is enforced with the understanding that the angle ϕ is restricted to the interval $0 < \phi < \alpha$. Introducing the nondimensional toughening parameter $\Lambda = K/K_m$, carrying out the integration with respect to dx_0, and regrouping eqn (7) results in the expression

$$1 = \Lambda\left(\frac{L}{R}\right)^{1/2}\cos(\phi/2) - \frac{\omega}{9\pi}\int_0^{\pi} M(\phi,\phi')\,\frac{dy_0(\phi')}{L} \qquad (14)$$

governing the active zone boundary $R(\phi)/L$. All distances in eqn (14) are measured from the crack tip and the integration extends over the entire boundary $0 < \phi' < \pi$.

The tip stress-intensity-factor can be maintained at K_m by enforcing eqn (13), which now requires

$$\Lambda = 1 + \frac{2\omega}{9\pi}\int_0^{\pi}\left(\frac{R}{L}\right)^{-1/2}\cos(\phi/2)\,\frac{dy_0(\phi)}{L} \qquad (15)$$

The system (14) and (15) constitute a nonlinear integral equation and a scalar equation for $R(\phi)/L$ and Λ. For the initial crack increment, (14), (15) and tangency conditions at α and β, can be solved for $R(\phi)/L$ in $(0 < \phi < \alpha)$, Λ, α and β. For a series of subsequent crack increments $R(\phi)/L$, Λ, and α are found repeatedly to generate the zone shape and the crack-growth resistance. The solution procedure for each crack increment is outlined in Appendix B.

Growing zone shapes for $\omega = 5$ and 10 are shown in Fig. 7. The dashed curves indicate the positions of active segments for various amounts of crack extension; the innermost curve is the initial boundary. The R-curves, plots of Λ versus $\Delta a/L$, for $\omega = 5,10$ along with their respective steady-state toughening asymptotes, as found by Budiansky and Amazigo (1987), are shown in Fig. 8. The results of Figs. 7 and 8 are quite unexpected. The zone height , H/L, and the

toughening, Λ, both overshoot their steady-state levels for finite amounts of crack advance before approaching them asymptotically from above.

The R-curves of Fig. 8 are qualitatively consistent with some available experimental measurements. A number of investigators, including Swain (1983), and Swain and Hannink (1984), have reported R-curves which exhibit peaks in toughness. However, the corresponding peak in zone height has not been reported. Even though the actual zone boundary between transformed and untransformed regions occurs over a diffuse region, the issue of zone widening should be explored experimentally.

R-curves and transformation-zones have been calculated for various values of ω, and the results for the peak toughening Λ_p and peak zone height H_p are shown in Table 1. Also shown are the crack extensions $\Delta a(\Lambda_p)$ and $\Delta a(H_p)$ necessary to reach each peak. Both Λ_p and H_p are seen to increase dramatically in the interval $19 < \omega < 20$. Denoting the steady state toughening ratio K_s/K_m, as calculated by Budiansky and Amazigo (1987), by Λ_s, we compare the toughening predictions for the steady state and growing crack calculations in Fig. 9, which shows $(\Lambda_s)^{-1}$ and $(\Lambda_p)^{-1}$ versus ω. The implication for a growing crack is "lockup" for ω greater than 20.4 . The steady state configuration (Fig. 1a) can not be reached from the growth of an initial zone for $\omega >$ 20.4 .

It may be noted from Fig. 8 that a tiny secondary maximum appears in the R-curve for $\omega = 10$. For values of ω greater than 10 (but less than 20.4) additional peaks of decreasing amplitude were found to appear in the R-curves as the toughness decayed in an oscillatory fashion to its steady-state magnitude.

By considering the initial slope of the R-curves, it is possible to define an initial tearing resistance parameter

$$t = \frac{d(K/K_m)}{d(a/L)} = \frac{E}{9\pi(\sigma_m^c)^2}\left(\frac{1+\nu}{1-\nu}\right)\frac{dJ}{da} \tag{16}$$

Here t represents the rate of toughening increase as the crack begins its initial growth and is plotted versus ω in Fig. 10. A comparison can be made with the approximate results of

Hutchinson (1986) who neglected the effect of the transformation on the zone boundary in his study of initial tearing resistance. Figure 11 shows a comparison of both sets of calculations for small ω. In the limit $\omega \to 0$, the predictions coincide.

CONCLUDING REMARKS

In the presence of transforming particles, the resistance to crack growth, as measured by the applied stress intensity K, reaches a maximum at a finite amount of crack growth. This maximum exceeds the steady-state toughness by an amount that varies with the transformation intensity parameter ω. Furthermore, "lock-up" (i.e. infinite toughening), occurs at a critical value of $\omega = 20.4$, which is substantially smaller than the value $\omega = 30$ corresponding to steady-state toughening. The potential benefits of transformation toughening must be assessed on the basis of transient crack growth since the steady-state condition seriously underestimates the toughening effect of transforming particles.

ACKNOWLEDGEMENTS

This work was supported in part by the DARPA University Research Initiative (Subagreement P. O. #VB38639-0 with the University of California, Santa Barbara, ONR Prime Contract N00014-86-K-0753), the Office of Naval Research (Contract N00014-84-K-0510), and the Division of Applied Sciences, Harvard University. The work of DMS was partially supported by a National Science Foundation Graduate Fellowship.

REFERENCES

J.C. Amazigo and B. Budiansky, Steady-state crack growth in supercritically transforming materials, Harvard University report MECH-107, 1987 (to be published in Int. J. Solids Structures).

B. Budiansky, J.W. Hutchinson and J.C. Lambropoulos, Continuum theory of dilatant transformation toughening in ceramics, Int.J. Solids Structures 19, pp 337-355 (1983).

A.G. Evans and R.M. Cannon, Toughening of brittle solids by martensitic transformations, Acta Metall. 34, pp. 761-800 (1986).

J.W. Hutchinson, On steady state quasi-static crack growth. Harvard University Report, Division of Applied Sciences, DEAP S-8, April 1974.

J.W. Hutchinson, Initial crack growth tearing resistance in transformation toughened ceramics. In Advanced Materials for Severe Service Applications (Edited by K. Iida), pp 77-90 (1987).

J.C. Lambropoulos, Shear, shape and orientation effects in transformation toughening, Int. J. Solids Structures 22, pp 1083-1106 (1986).

R.M. McMeeking and A.C. Evans, Mechanics of transformation toughening in brittle materials, J. Am. Ceram. Soc. 69, pp 242-246 (1982).

L.R. F. Rose, A kinematical model for stress -induced transformation toughening in brittle materials, J. Am. Ceram. Soc. 34, pp 208-211 (1986a).

L.R.F. Rose, The size of the transformed zone during steady-state cracking in transformation-toughened materials, J. Mech. Phys. Solids 34, pp 609-616 (1986b).

M.V. Swain, R-curve behavior of magnesia-partially-stabilized zirconia and its significance for thermal shock. In Fracture Mechanics of Ceramics (Edited by R.C. Bradt et al.), Vol. 6, pp 355-370 (1983).

M.V. Swain and R.H.J. Hannink, R-curve behavior of zirconia ceramics. In Advances in Ceramics (Edited by N. Claussen), Vol. 12, pp 225-239 (1984).

APPENDIX A

The initial zone boundary, $R(\phi)$, can be found by solving the nonlinear integral equation (8). However before proceeding, it is instructive to examine the solution for $\omega = 0$ given by eqn (3) and shown in Fig. 3:

$$R(\phi) = L[1/2 + 1/2 \cos(\phi)] \tag{A1}$$

Due to Mode-I symmetry, the boundary at $\phi = 0$ intersects the axis ahead of the tip normally. However, at $\phi = \pi$, the boundary runs through the crack tip tangentially to the crack face.

For $\omega \neq 0$, the possibility that the boundary at $\phi = \pi$ detaches from the crack tip must be admitted. An analysis of the integral in eqn (8) shows that if $R(\pi) \neq 0$, the boundary intersects the crack faces normally. An expansion for $R(\phi)$ meeting the boundary requirements at 0 and π is

$$R(\phi) = \sum_{n=0}^{N} a_n \cos(n\phi) \tag{A2}$$

Substitution of equation (A2) allows eqn (8) to be rewritten in the form,

$$G(a_0,a_1,\ldots,a_N,\phi) - 1 = 0 \tag{A3}$$

where the function G is the right hand side of eqn (8).

In this study, the solution for the (N+1) unknown coefficients was accomplished by collocating eqn (A3) at N+1 equally spaced points, $\phi = \pi n/(N+1)$ where $n = (0,1,2,\ldots,N)$, in the interval $0 < \phi < \pi$. A Newton-Raphson iterative technique was then used to solve for the N+1 unknown coefficients. The integral in eqn (A3) was evaluated by Gaussian quadrature. Convergence was assumed when the relative change in successive iterations of each of the unknowns was less than 0.001. For the initial zones shown in Fig. 3, it was found that a 10 term expansion was sufficient to obtain a highly accurate solution. As an additional check on the accuracy of the overall shape, the constraint on $R(\phi)/L$, eqn (13) with $K_{tip}/K = 1$, was evaluated and found to hold to within 10^{-5} for each of the zones of Fig. 3.

APPENDIX B

The solution for the unknowns $R(\phi)$, α, and Λ after a typical crack increment (Fig. 6b) involves solving the integral equation (14), the scalar equation (15), and meeting the tangency condition

$$\frac{dy}{dx}(B)\Big|_{passive} = \frac{dy}{dx}(B)\Big|_{active} \tag{B1}$$

For the initial crack increment the system must be supplemented with the unknown β and the additional tangency equation

$$\frac{dy}{dx}(C)\Big|_{passive} = \frac{dy}{dx}(C)\Big|_{residual} \tag{B2}$$

An appropriate expansion for the radius of the instantaneous active segment which meets Mode-I symmetry conditions is

$$R(\phi) = \sum_{n=0}^{N} a_n T_{2n}(\phi/\alpha) \tag{B3}$$

where the T_{2n} are the even Tchebyshev polynomials. Substituting this expression into (14), (15), and (B1) results in a set of equations for the unknowns $(a_0, a_1, \ldots, a_N)$, α, and Λ.

The solution procedure will be described for the general growth increment as shown in Fig. 6b. For the initial increment, the process is the same with β and (B2) added to the list of unknowns and equations. For a given Δa, a system of N+3 equations was generated by enforcing equations (15), (B1), and collocating eqn (14) at N+1 equally spaced points $\phi = n\alpha/(N+1)$ $(n=0,1,2,\ldots,N+1)$. The equations were written in residual form and Newton-Raphson method was used to find the solution. Gaussian quadrature was used to evaluate the integrals in eqns (14) and (15). Convergence to a solution was specified by a relative change of less than 0.001 between iterations. A 6 term expansion for $R(\phi)$ was found sufficient to obtain a solution at all stages of growth.

Initial growth increments had to be small, $< 0.05/L$, to capture the early zone shape. As crack extension proceeded, it was found that the increment size could be increased. The number of increments necessary to grow the crack to peaks in height and toughening varied greatly. For

small values of ω less than 50 increments were sufficient. However for values of ω between 17 and 20, several hundred increments were necessary to reach H_p and Λ_p. During the growth process, the mean stress exterior to the zone was checked to confirm that it was less than σ_m^c. The final results shown herein were checked by calculations with the increment steps halved.

TABLE 1

ω	Λ_p	H_p/L	$\Delta a(\Lambda_p)$	$\Delta a(H_p)$
5	1.29	1.03	5.5	2.4
10	1.80	1.91	10.25	5.6
15	3.07	5.17	29.4	18.4
17.5	5.06	13.6	81.0	55.0
19.5	16.3	351	2400	1875
20.0	74.3	2764	20,200	15,900

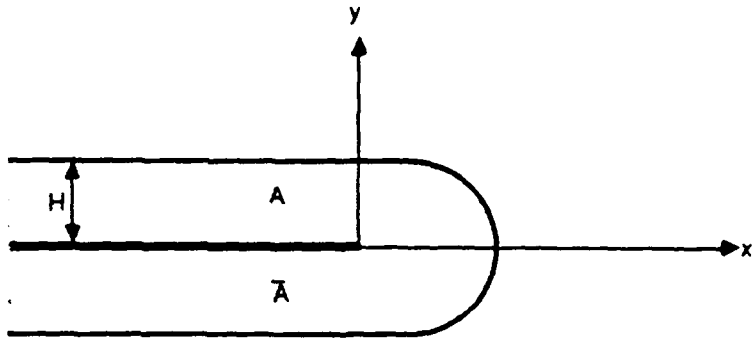

Fig. 1a Steady-state transformation zone surrounding a crack tip

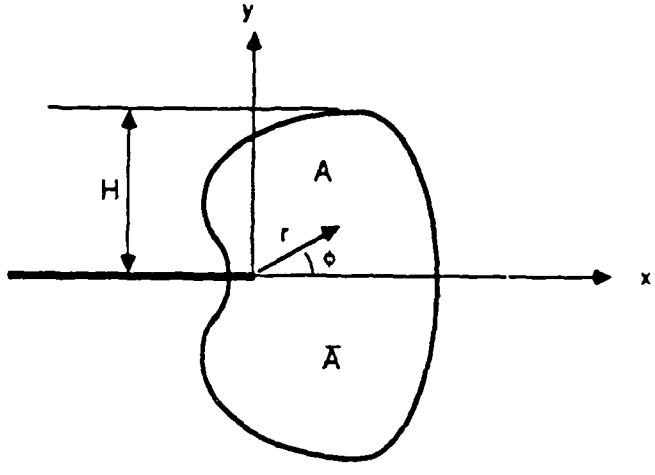

Fig. 1b Initial transformation zone around a stationary crack

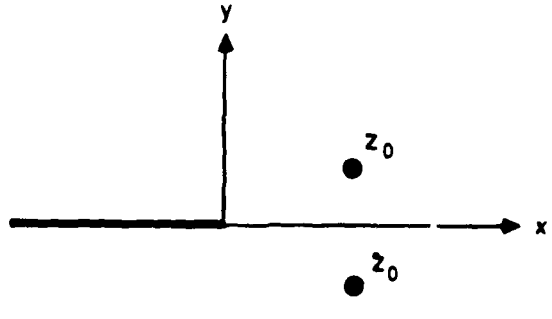

Fig. 2 Symmetrically located spots of dilatation

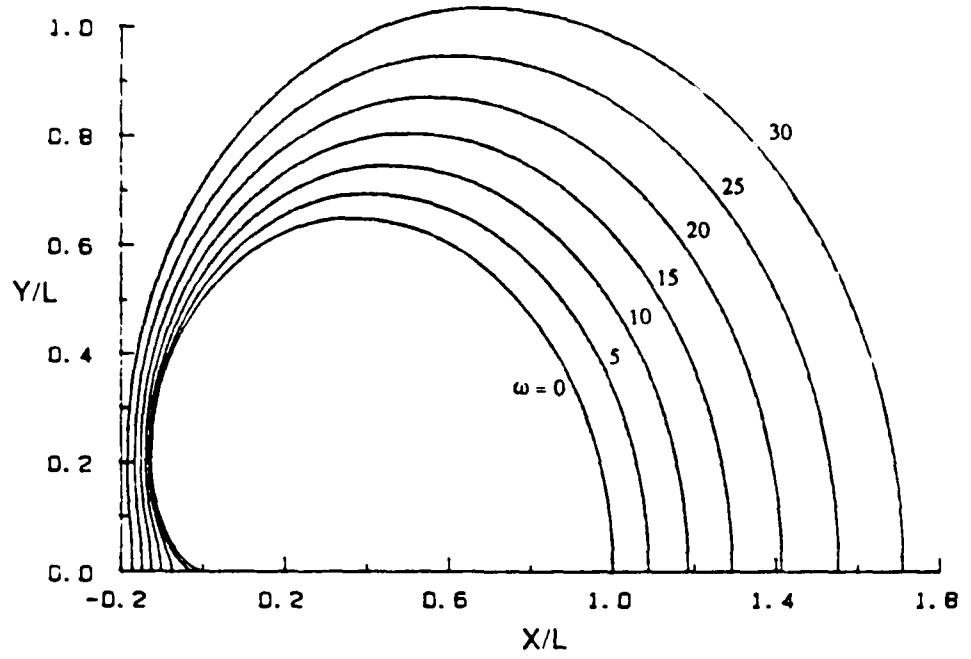

Fig. 3 Initial transformed zones for various ω

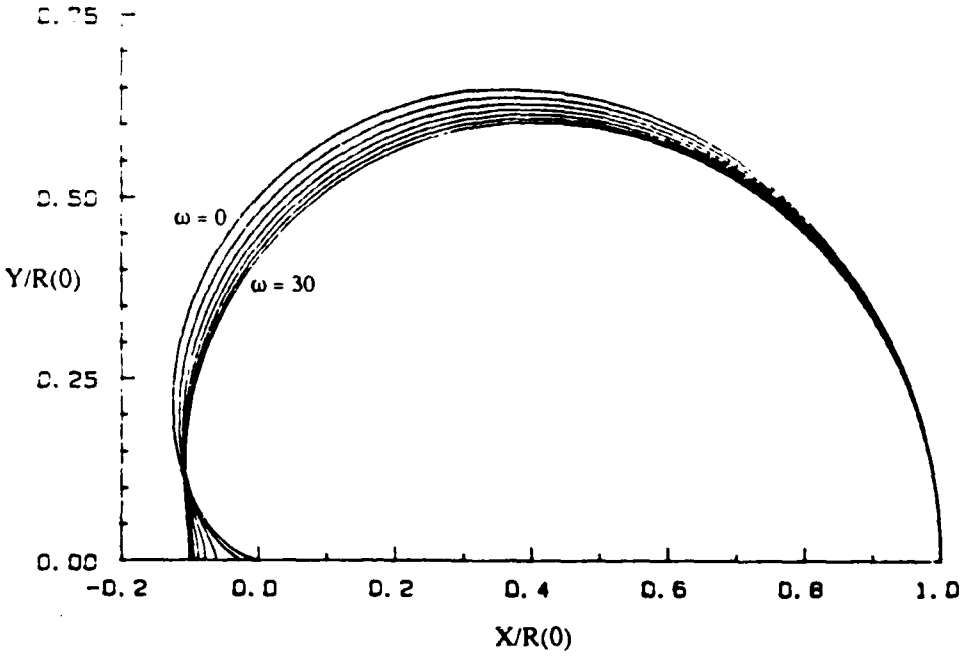

Fig. 4 Initial transformed zones normalized by frontal intercept length

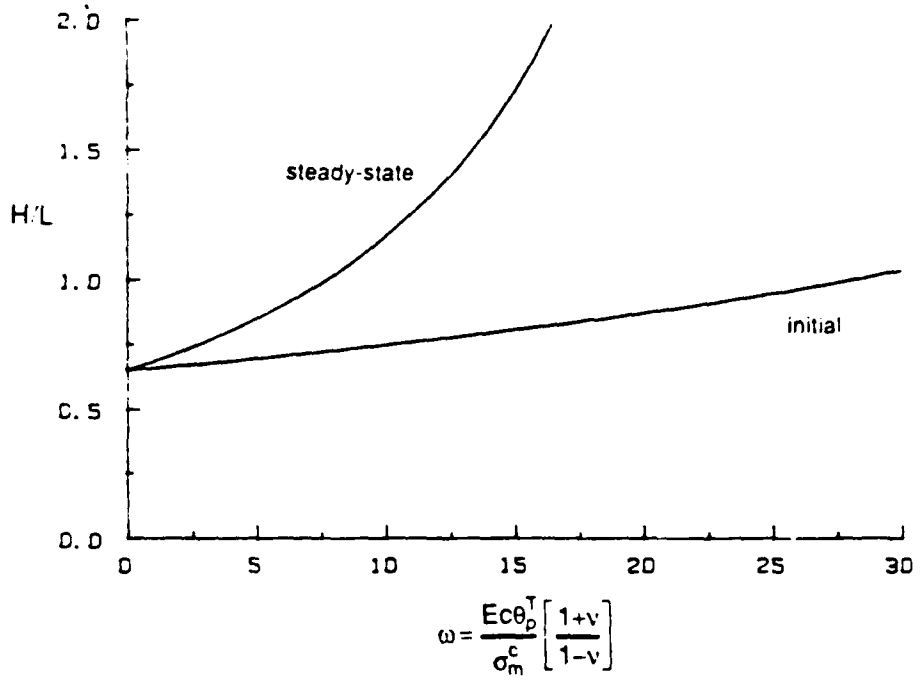

Fig. 5 Steady-state and initial zone heights versus ω

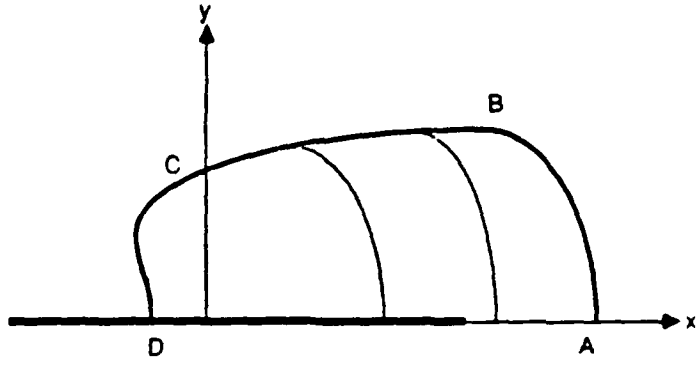

Fig. 6a Transformation zone around a growing crack

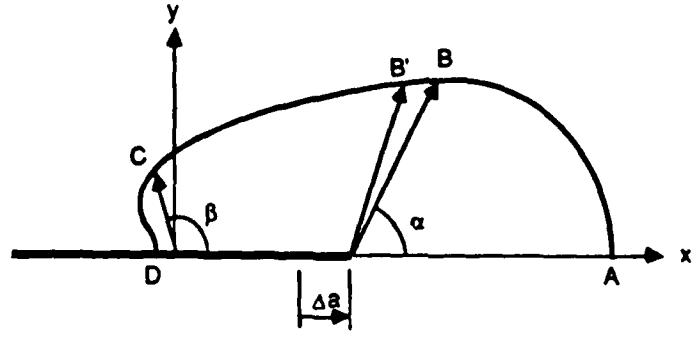

Fig. 6b Zone extension model used to find the instantaneous active zone and passive segment growth

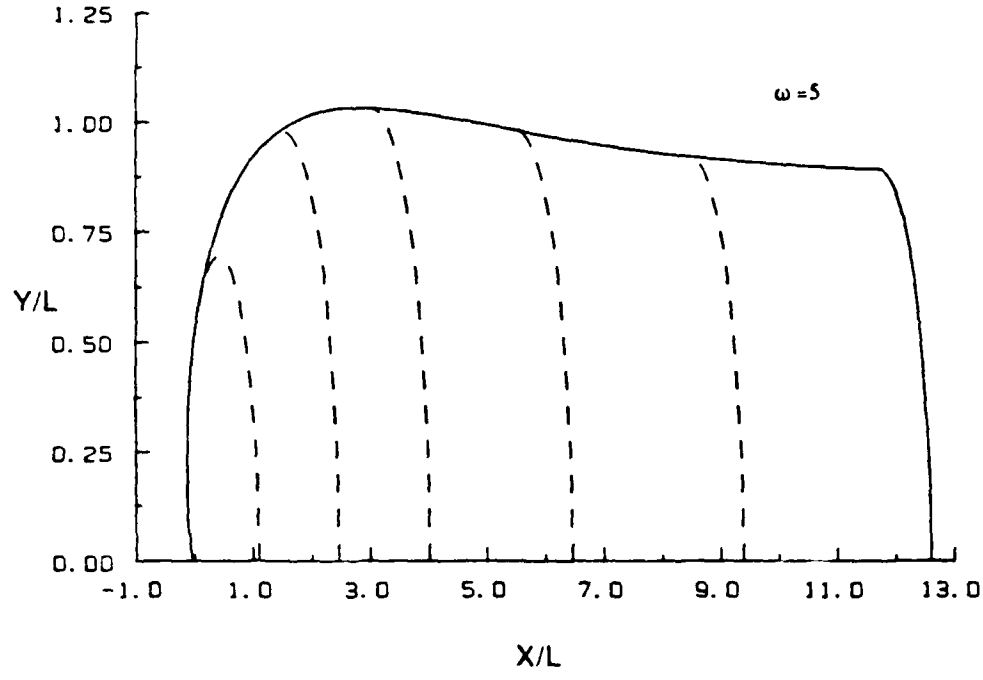

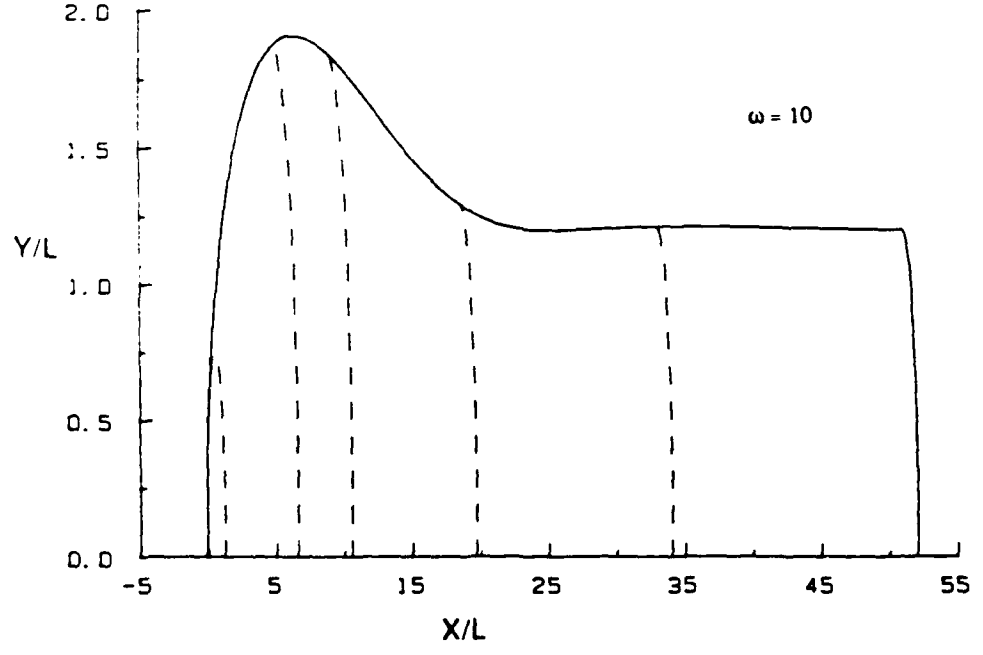

Fig. 7 Growing zones for $\omega = 5,10$

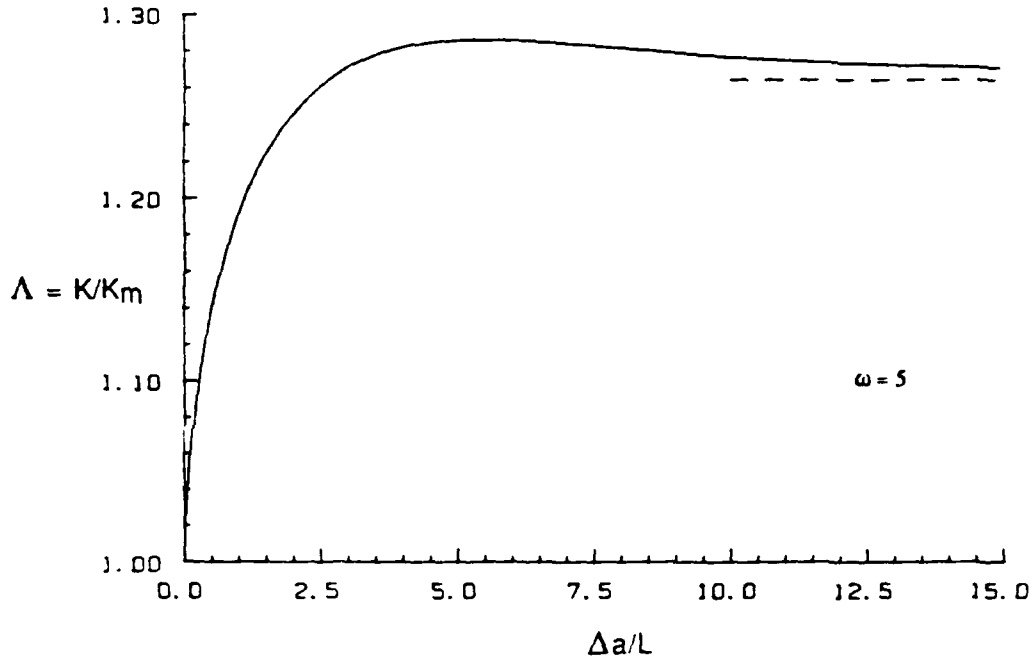

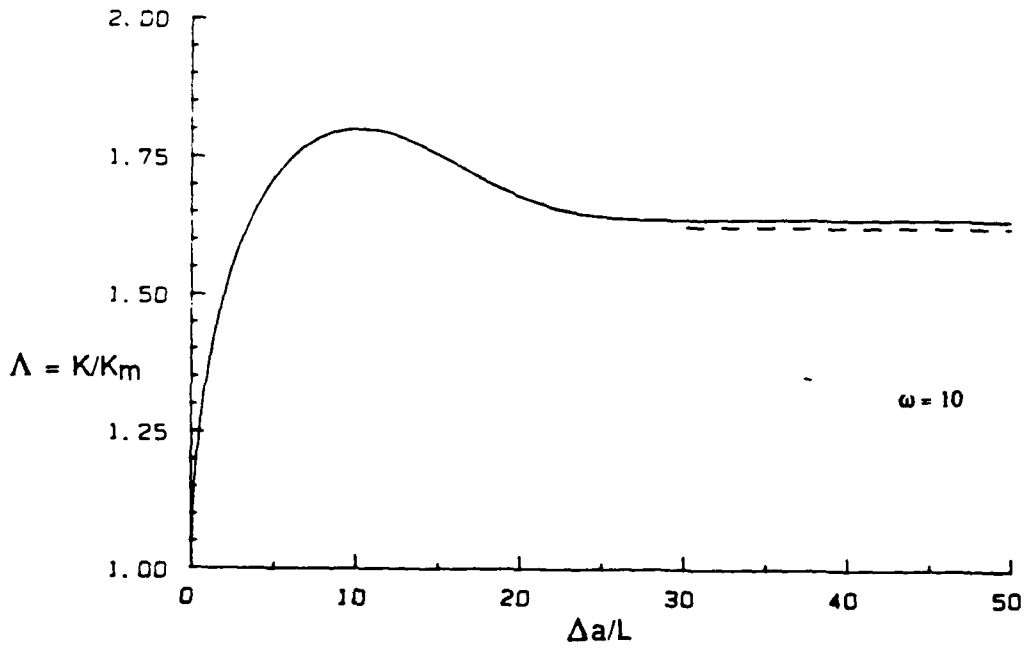

Fig. 8 Resistance curves for $\omega = 5,10$

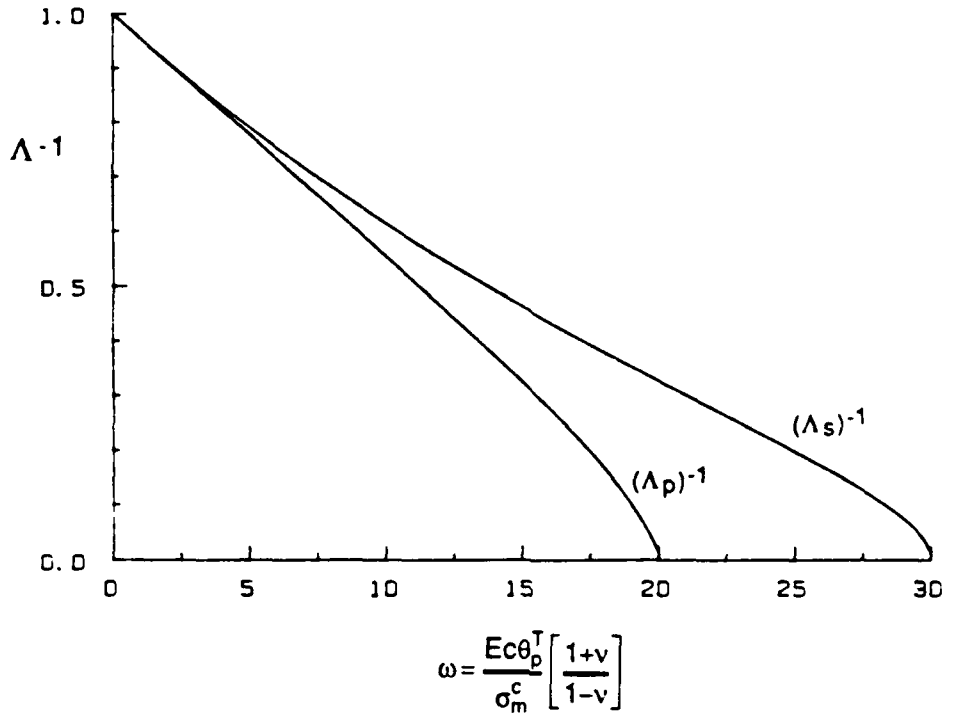

Fig. 9 Reciprocal of peak and steady-state toughening versus ω

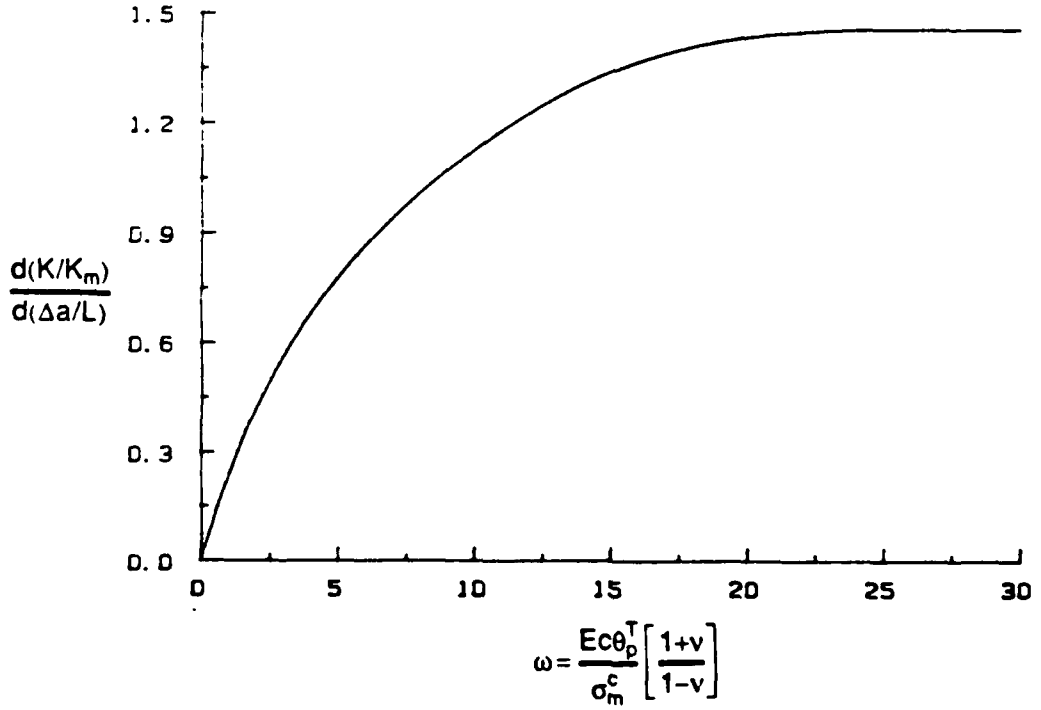

Fig. 10 Initial crack-growth resistance versus ω

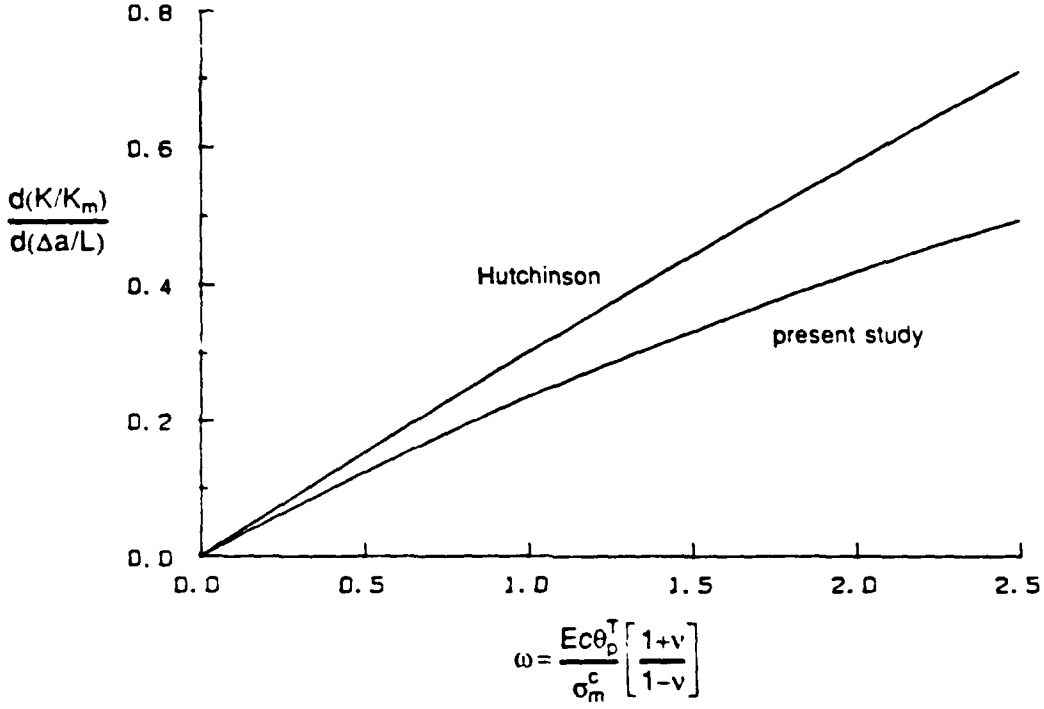

Fig. 11 Comparison with Hutchinson's (1986) results for initial crack-growth resistance